

***K-K*-electron transfer and *K*-shell-vacancy production cross sections for Ti bombarded by ^{28}Si and ^{32}S beams at 1.25–4.70 MeV/amu**

L. C. Tribedi, K. G. Prasad, and P. N. Tandon

Tata Institute of Fundamental Research, Bombay 400 005, India

(Received 23 December 1992)

Single and double *K-K*-electron transfer and the *K*-shell-vacancy production cross sections for Ti bombarded by ^{28}Si and ^{32}S beams at energies varying between 1.25 and 4.7 MeV/amu have been determined, in the limit of zero target thickness, from the thickness variation of the Ti *K* x-ray yield with ion beams having 0, 1, or 2 vacancies in their *K* shell. From the measured energy shift and the intensity ratios of *K α* , *K β* lines, the average number of *2p* and *3p* vacancies were determined from which the average value of the fluorescence yield ω_K was deduced using the statistical scaling procedure of Larkins [J. Phys. B **4**, L29 (1971)]. The single-electron transfer cross sections are compared with the calculations of Brinkman and Kramer as formulated by Nikolaev [Sov. Phys. JETP **24**, 847 (1967)] and those of Lapicki and McDaniel [Phys. Rev. A **22**, 1896 (1980)] and the modified two-center atomic-orbital-expansion model (AO+) of Fritsch and Lin [J. Phys. B **15**, 1255 (1982)]. The double-electron transfer cross sections are also compared with the AO+ predictions. The *K*-shell-vacancy production data are compared with calculations based on the perturbed-stationary-state approach with the Coulomb-deflection, binding-energy, and relativistic corrections (ECPSSR) included. In addition, the projectile cross sections for single-electron capture and loss have also been deduced at a few energies.

PACS number(s): 34.50.Fa, 34.70.+e

I. INTRODUCTION

Extensive measurements on the *K*-shell ionization of elements by proton and α -particle beams have been made in the past [1]. Recently the interest in this area has been renewed and systematic measurements of the cross sections for low-*Z* elements ($6 \leq Z \leq 22$) using proton and ^4He beams have been reported [2–4]. The *K*-shell ionization, in these cases, is mainly due to direct Coulomb interaction between the projectile ion and target electrons and are quantitatively described by the perturbed-stationary-state theory (PSS) in which the effects due to the energy (*E*) loss of the projectile during the collision, Coulomb (*C*) deflection of the projectile in the field of the target nucleus, and relativistic (*R*) electron motion (ECPSSR) are incorporated in the plane-wave Born approximation [5]. When heavy ions are used as projectiles, the electron transfer from the target *K* shell to the unoccupied states in the projectile also contribute to the target-*K*-vacancy production. These cross sections are particularly large when completely stripped ions are used as projectiles [6]. Tanis *et al.* [7] have measured the *K*-shell x-ray production cross sections in K, Ti, Mn, and Br using Cl beams with no *K*-shell vacancy, thus suppressing the contribution from the *K-K*-electron transfer channel. They find reasonable agreement with the ECPSSR theory for $Z_1/Z_2 \approx 0.5$ (here the subscripts 1 and 2 refer to the projectile and the target, respectively) while the agreement becomes progressively worse as Z_1/Z_2 approaches unity, even when $v_1/v_{2K} \approx 0.3$ (v_1 is the projectile velocity and v_{2K} the mean velocity of the target *K* electrons).

The relative importance of direct ionization and electron transfer in *K*-shell ionization by heavy ions has been extensively investigated for Ti bombarded with a number

of heavy ion beams up to Cl and over a wide energy range of 0.5 to 6.5 MeV/amu [8,9]. These investigations show that direct ionization plays a dominant role for the asymmetric collision system ($Z_1/Z_2 \leq 0.4$) at low to intermediate collision velocities ($v_1/v_{2K} \leq 0.8$). As the collision system becomes more symmetric electron transfer from the target *K* shell to the projectile plays an increasingly important role in the *K*-vacancy formation by the projectile.

The previously reported data for the Cl beam on Ti in Ref. [7] were measured using a single target of thickness $3.9 \mu\text{g}/\text{cm}^2$. The existing data for Ti with various ion beams in Refs. [8,9] are for a vanishing thin (about $1 \mu\text{g}/\text{cm}^2$) target though the thickness variations were not investigated. We report in this work systematic measurements of single and double *K-K*-electron transfer and the *K*-shell-vacancy production cross sections in nearly symmetric collision systems of Ti bombarded by ^{28}Si ($Z_1/Z_2 = 0.66$) and ^{32}S ($Z_1/Z_2 = 0.73$) beams. The experiments were performed at a few energies in the range of 1.25 to 4.7 MeV/amu (v_1/v_{2K} varying from 0.24 to 0.73). The target cross sections were extracted, in the limit of zero target thickness, from the variation of the target x-ray yield with thickness in order to avoid target thickness effects [6]. Sulfur beams having zero, one, or two initial vacancies in their *K* shells were used in the measurements. Earlier measurements on this collision system were restricted to 0.5–2.25 MeV/amu of S [9]. We have also measured these cross sections for Ti using Si beams in a similar energy range.

The electron transfer cross sections can be calculated in the Oppenheimer-Brinkman-Kramer (OBK) approximation as formulated by Nikolaev (OBKN) [10]. These calculations overestimate the capture cross sections and

semiempirical scaling factors have to be used to find agreement with the measured values. Lapicki and McDaniel [11] have developed formulas for electron capture from inner shells of target atoms by fully stripped ions and have also included the second Born term and effects of binding energy and Coulomb deflection in the OBKN formalism. They have shown that reliable cross sections for electron transfer can be obtained without the use of semiempirical scaling factors. More rigorous *ab initio* calculations in the two-state atomic-expansion (TSAE) model have been developed by Lin and Tunnell [12] to describe the K - K -electron transfer cross sections. A modified two-center atomic-orbital-expansion (AO+) method has also been proposed by Fritsch and Lin [13,14] to calculate the K - K transfer cross sections. In this method, in addition to the atomic orbitals of the separated atoms, the united-atom orbitals are also included in the two-center expansion to calculate the cross sections in the low-to-intermediate energy region. The capture cross sections deduced in the present work are compared with the predictions of these models.

II. EXPERIMENTAL DETAILS

The experimental setup used in this work has been described earlier [3,15] and hence only a brief outline will be provided. ^{32}S (40–150 MeV) and ^{28}Si (39–125 MeV) beams were obtained from the BARC-TIFR Pelletron accelerator at Bombay. The mass and energy analyzed beam was passed through a carbon foil stripper [16] to obtain different charge states of the incoming beam. The charge selected beam from the switching magnet was then directed into an electrically isolated chamber and dumped 50 cm away from the target. The whole chamber, including the beam dump, was used for charge collection. Thin targets of Ti of thicknesses varying between 1 and 20 $\mu\text{g}/\text{cm}^2$ were prepared on carbon backings of 10 $\mu\text{g}/\text{cm}^2$ by vacuum evaporation. The thicknesses of these targets were obtained during the measurement from the Rutherford scattering of S and Si beams at the lowest bombarding energy used. The targets were mounted on a rotatable multiple target holder [17] and were kept at 45° with respect to the beam direction. The emerging beam from the target was scattered from a gold foil of known thickness mounted 6 cm downstream. The scattered particles were detected at 120° in a Si surface-barrier detector. This provided an independent normalization of the beam. The emitted x rays were detected in two Si(Li) detectors (with a 25- μm Be window and 170-eV resolution at 5.9 keV) mounted face to face outside the scattering chamber in air at 90° to the beam direction. The efficiency of the detectors was measured earlier [18]. The total count rate in each detector was kept below 600 counts/s for Si and 1000 counts/s for S by using suitable absorbers of known thickness to reduce the predominant projectile x rays.

III. DATA ANALYSIS AND RESULTS

A typical x-ray spectrum recorded in the region of Ti K x rays is shown in Fig. 1. The $K\alpha$ and $K\beta$ components, due to the decay of the single- K -vacancy state,

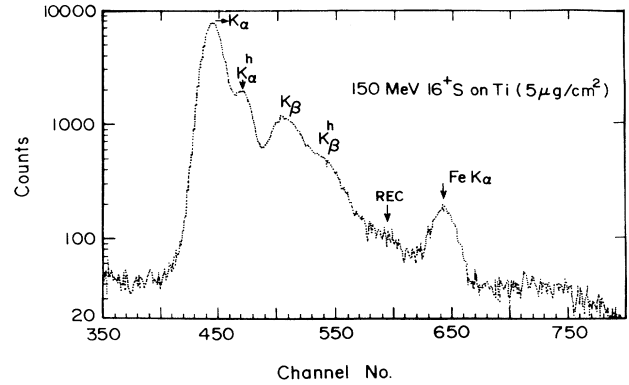


FIG. 1. A typical spectrum showing the Ti $K\alpha$, $K\alpha^h$, $K\beta$, $K\beta^h$ x rays and the REC peak obtained for the ^{32}S beam of 150 MeV. The small Fe $K\alpha$ peak is due to the scattering from the target frame made of stainless steel.

as well as hypersatellite components $K\alpha^h$ and $K\beta^h$, due to the decay of double- K -vacancy states, are clearly seen and resolved. The hypersatellite components are more pronounced when completely stripped ion beams are used. The underlying background in this region is due to the pileup of projectile x rays and from the broad REC (radiative-electron-capture) peak whose position varied as a function of the beam energy used. The REC background was very small and subtracted from the measured spectra using a carbon target of appropriate thickness (also see Ref. [15]). The intensities of the satellite and hypersatellite components were obtained from a fit to the composite spectrum using a Gaussian peak shape and a linear background and were corrected for the absorber thickness. The normalized yields were used for further analysis.

To compare the observed x-ray production cross sections with the theoretical models they have to be converted into ionization cross sections. The K ionization cross section (σ_{KI}) was deduced from the measured K x-ray production cross-section (σ_{KX}) data by using the following relation:

$$\sigma_{KI} = \sigma_{KX} / \omega_K(E, \delta), \quad (1)$$

where $\omega_K(E, \delta)$ denotes the fluorescence yield as a function of beam energy (E) and the parameter δ represents the dependence of fluorescence yield on the electron configuration of the target atom emitting x rays. The single hole fluorescence yield as provided by Krause [19] are inadequate for the present case since one has to consider multiple ionization of the outer shells of the target atoms caused by heavy ion impact. To calculate the fluorescence yield in such cases one has to know the atomic configuration of the target atom at the instant of x-ray emission. We have derived the average number of vacancies in the $2p$ and $3p$ shells at the time of x-ray emission from the measured intensity ratios of the $K\beta$ and $K\alpha$ components and the changes in their energy as compared to the theoretical values corresponding to single vacancy. The intensity ratios and the energy shifts are shown in Fig. 2 as a function of the beam energy. As can be seen

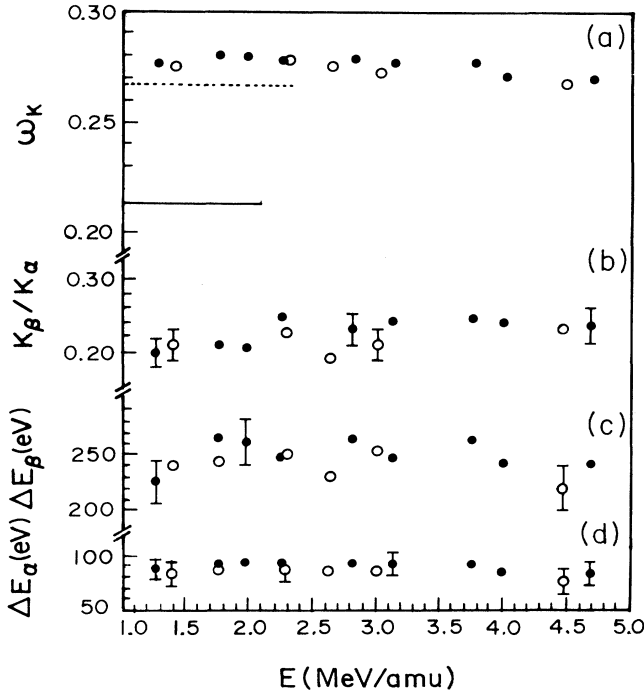


FIG. 2. The energy shift of Ti $K\alpha$ (ΔE_α) (d) and $K\beta$ (ΔE_β) (c) x rays along with the intensity ratio ($I_{K\beta}/I_{K\alpha}$) (b). The derived values of ω_K for Ti are shown for both the ^{28}Si and ^{32}S beams (a). The value of ω_K (0.27) as measured by Tanis *et al.* [7] for Ti using chlorine beam is shown by a dotted line. The single-hole value of ω_K (0.214) [19] is shown as a solid horizontal line.

from the figure, in the energy range investigated here, there is no appreciable change in these quantities with the beam energy. The observed intensity ratio $I(K\beta)/I(K\alpha)$ is found to vary between 0.20 to 0.25 as compared to a value of 0.13 calculated by Scofield [20] indicating thereby the presence of multiple ionization affecting x-ray

emission. Hartree-Fock calculations have been used [7] to derive the number of $2p$ vacancies from the measured energy shift. The average number of $3p$ vacancies are obtained from the intensity ratios of the $K\beta$ and $K\alpha$ x rays and the derived values of $2p$ vacancies (see Ref. [7] for details). The value of the fluorescence yield ω_K is then derived using the statistical procedure of Larkins [21,6]. The calculated values are shown in Table I. It is seen that the calculated values are almost constant (within about 3%) over all the energies (see Fig. 2). There is no appreciable variation between the values for S and Si projectiles. A similar constant value (0.27) of ω_K for Ti using a Cl beam was reported by Tanis *et al.* [7]. The ω_K values as estimated by Hall and co-workers [8,9,22], from the available high-resolution x-ray data of Sc induced by heavy ions, are about 10% lower with respect to our values. All the x-ray production cross-section (σ_{KX}) data were converted to ionization cross sections (σ_{KI}) by using the measured value of ω_K which was found to be independent of target thickness and the initial charge states of the beam.

Figure 3 shows a few typical data sets showing variation of the total target K -ionization cross sections (σ_{KI}) with the target thickness for different initial charge states of the beam corresponding to 0, 1, or 2 K vacancies. This thickness dependence arises due to the changing fraction of the ions with K -shell vacancies as a consequence of the continuing electron capture and loss processes which are operative as the projectile moves through the foil. The state of the projectile K shell, as a function of the target thickness x , can be described by a set of rate equations in a three-component model [23]. The solutions of these rate equations give the probability that the projectile will have a single [$F_1(x)$] and double [$F_2(x)$] K vacancy after traversing the thickness x and can be written in the form [6,15,23,24]

$$F_j^i(x) = [F_j(\infty) + P_j^i e^{qx} + N_j^i e^{-qx}] e^{-\frac{1}{2}x\Delta\sigma_{if}}, \quad (2)$$

TABLE I. The single- K -vacancy cross sections of Ti for ^{28}Si and ^{32}S beams. All cross sections are in units of Mb. The single K - K -electron transfer cross sections (σ_{SKV}^{K-K}) in column 7 are derived from σ_{SKV}^0 and σ_{SKV}^1 using $\kappa=0.5$ [see Eq. (7)]. The same quantities in column 8 are obtained from the difference, $\sigma_{SKV}^2 - \sigma_{SKV}^0$. The average errors in σ_{SKV}^0 and σ_{SKV}^{K-K} are about 20% and 30%, respectively. Typical error in ω_K is about 5%.

Beam	E (MeV/amu)	ω_K	σ_{SKV}^0	σ_{SKV}^1	σ_{SKV}^2	σ_{SKV}^{K-K}	σ_{SKV}^{K-K}
Si	1.39	0.275	0.022	0.179		0.314	
	1.75	0.281	0.044	0.179		0.464	
	2.26	0.279	0.085	0.420		0.670	
	2.57	0.276	0.114	0.540		0.852	
	3.00	0.274	0.130	0.523	0.839	0.786	0.708
	4.46	0.271	0.234	0.701	0.994	0.934	0.760
	4.69	0.273	0.328	1.645	1.767	2.21	1.439
S	1.25	0.276	0.025				
	1.75	0.280	0.062				
	1.97	0.280	0.090	0.900		1.62	
	2.25	0.279	0.128	0.897		1.54	
	2.81	0.280	0.235	1.308		2.15	
	3.13	0.278	0.173	0.772		1.20	
	3.75	0.279	0.212	1.220		1.70	
	4.00	0.273	0.296	1.278	1.335	1.63	1.123
	4.00	0.273	0.296	1.278	1.335	1.63	1.123
	4.69	0.273	0.328	1.645	1.767	2.21	1.439

where i is the *initial* number of K vacancies present in the beam and $F_j^i(x)$, ($j=0,1,2$), denote the probability for the projectile to have j vacancies in the K shell after traversing a thickness x . The quantities p_j^i , N_j^i , q , Δ , and $F_j(\infty)$ are functions of σ_{jf} ($j, f=0,1,2$) where σ_{jf} represent the electron capture ($j > f$) and loss ($j < f$) cross sections for transition from a state with j K vacancies to a state with f K vacancies in the projectile and their functional form can be found from Ref. [23]. Therefore the average target K x-ray production cross section (σ_{KX}) can be written in terms of the contribution from the individual projectile K -vacancy fractions as

$$\sigma_{KX}^i = \frac{\sigma_{K0}}{x} \int_0^x [1 + (\alpha - 1)F_1^i(x) + (\beta - 1)F_2^i(x)] dx, \quad (3)$$

where $F_1^i(x)$ and $F_2^i(x)$ are given by Eq. (2). The quantities α and β represent the enhancement of the target K x-ray yield (in the zero thickness limit) for an incident beam with single and double K vacancies over that with zero K vacancy and are expressed by the following relations:

$$\alpha = \sigma_{K1}/\sigma_{K0} \text{ and } \beta = \sigma_{K2}/\sigma_{K0}. \quad (4)$$

The quantities σ_{K0} , σ_{K1} , and σ_{K2} are the zero thickness values of target K x-ray production cross sections for projectiles incident with initial charge states having 0, 1, or 2

K vacancies, respectively. The x-ray cross-section data were fitted to Eq. (2) simultaneously for all the charge states measured at a given energy. Figure 3 shows such fits for S and Si beams at three energies. At each energy the data for different charge states were fitted simultaneously. It should be stressed here that the prime motivation of the fitting to the three-component model was to deduce the cross sections in the zero thickness limit. This method also provided information about the projectile cross sections σ_{jf} which are used as variable parameters for the fitting. However, the extraction of reliable values of all six cross sections from such a complicated fitting procedure is difficult, as has been discussed in detail by Schmiedekamp *et al.* [25]. The number of independent parameters, in the present fitting procedure, was reduced by using the following approximations.

(i) The two-electron capture and loss cross sections, σ_{20} and σ_{02} , are assumed to be negligible in comparison to the corresponding cross sections for single electrons ($\sigma_{01}, \sigma_{10}, \sigma_{12}$, and σ_{21}).

(ii) The capture or loss cross sections of a K electron are proportional to the number of vacancies or electrons, respectively, present in the K shell, i.e., $\sigma_{01} = 2\sigma_{12}$ and $\sigma_{21} = 2\sigma_{10}$. This procedure reduced the number of independent parameters to five, namely, three target cross sections and two projectile cross sections among which the target cross sections were relatively fixed and allowed to vary around the measured data for the thinnest ($\approx 1 \mu\text{g}/\text{cm}^2$) target. At lower energies where the double vacancies in the projectile are negligibly small, it was sufficient to use only the two-component model.

The data presented in Fig. 3 represent the total Ti K ionization cross sections deduced from total K x-ray production cross sections. These data also include the contributions from $K\alpha^h$ and $K\beta^h$ which were significant for beam energies $E_1 \geq 3 \text{ MeV}/\text{amu}$. In heavy ion atom collisions a significant number of double K vacancies are also created in the target. Their contribution should be known in order to obtain single ionization cross sections from the measured x-ray cross sections. This was done, from the total $K\alpha$ peak intensity by separating the $K\alpha$ satellite and hypersatellite contributions. Assuming the fluorescence yield for single- and double- K vacancy states to be similar [8,9], the corresponding single- and double- K -vacancy cross sections σ_{SKV}^i and σ_{DKV}^i are derived using the following relations:

$$\sigma_{DKV}^i = \sigma_{KI}^i \frac{N_\alpha^h}{N_\alpha(\text{tot})} \quad (5)$$

and

$$\sigma_{SKV}^i = \sigma_{KI}^i - 2\sigma_{KI}^i(H) \quad (6)$$

where $N_\alpha^h/N_\alpha(\text{tot})$ is the fraction of hypercomponent in the total $K\alpha$ x ray. Here the superscript i refers to the number of vacancies in the incident beam (0,1, or 2). The quantity $\sigma_{KI}^i(H)$ corresponds to the double- K -vacancy production cross section deduced from the hypersatellite intensity. From these the single and double K - K -electron transfer cross sections are obtained from the following relations [8,9]:

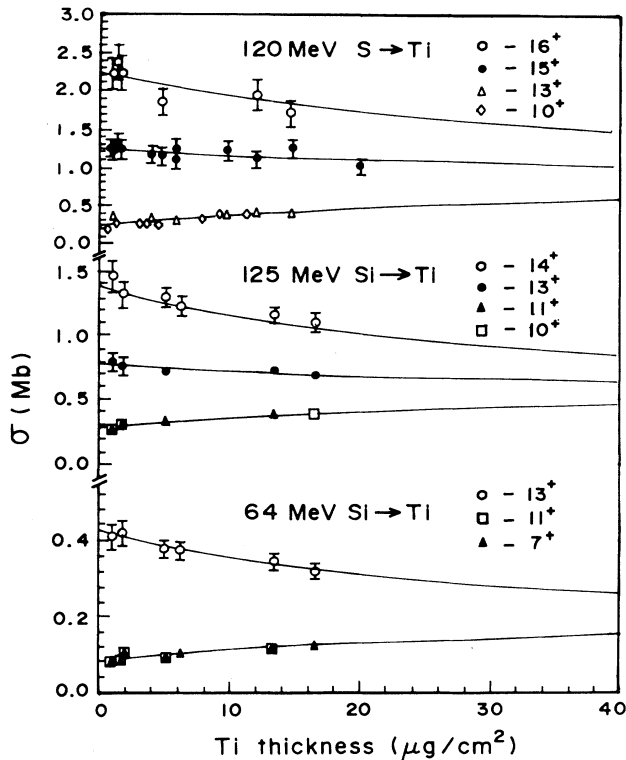


FIG. 3. The thickness dependence of the Ti K -shell ionization cross sections for the ^{28}Si and ^{32}S beams at a few energies. These ionization cross sections were deduced from the total x-ray production cross sections using the measured values of ω_K .

$$\sigma_{SKV}^{K-K} = \sigma_{SKV}^2 - \sigma_{SKV}^0 = \frac{(\sigma_{SKV}^1 - \sigma_{SKV}^0)}{\kappa} \quad (7)$$

and

$$\sigma_{DKV}^{2K-2K} = \sigma_{DKV}^2 - 2\sigma_{DKV}^1 + \sigma_{DKV}^0, \quad (8)$$

where κ is given by the following equation:

$$\kappa = \frac{(\sigma_{SKV}^1 - \sigma_{SKV}^0)}{(\sigma_{SKV}^2 - \sigma_{SKV}^0)}. \quad (9)$$

From the measured data at various energies κ was found close to 0.5. This value is also expected from the statistical point of view. We have used a value of 0.5 for κ [8,9] in order to deduce σ_{SKV}^{K-K} at lower energies where fully stripped beams were not available. This is quite a reasonable assumption as can be seen from the agreement of the σ_{SKV}^{K-K} data deduced from single-electron ions (open circle data in Figs. 4 and 5) as well as the fully stripped ions (open triangle data in Figs. 4 and 5). The cross-section values obtained are shown in Figs. 4 and 5 for Si and S data, respectively. The average error in the σ_{K0} and σ_{SKV}^{K-K} are about 20% and 30%, respectively. The average error in σ_{DKV}^{2K-2K} was estimated to be about 33%. These errors include the error in target thickness, detector efficiency, charge normalization, fluorescence yield, background subtraction (REC and pileup), and the fitting procedure to find the area. Each of these contribution varies from 5% to 10%. Our measured values for ^{28}Si and ^{32}S projectiles agree quite well with the earlier measurements though the Si data of Hall *et al.* [8] are systematically lower than ours by about 10–20%.

The derived values of the cross sections σ_{SKV}^0 and σ_{SKV}^{K-K} are shown in Figs. 4 and 5 and in Table I. The calculations based on the plane-wave Born approximation (PWBA) (not shown) overestimate the σ_{SKV}^0 throughout the energy range investigated. The ECPSSR calculations, on the other hand, underestimate the S data below $v_1/v_{2K}=0.4$ (2 MeV/amu) and overestimate it above 0.5 (3 MeV/amu). For Si it was found to agree with the data for $1.4 \leq E \leq 2.4$ MeV/amu. The crossover was found to be approximately at the same energy per nucleon (i.e., at $E/A \approx 2$ MeV/amu) for both the collision systems. Considering the fact that these calculations are valid for more light and asymmetric systems, the disagreement is not very surprising. Similar observations were made earlier from measurements involving asymmetric collision systems [7,8].

The K-K-electron transfer cross sections can be compared with the theoretical models for capture cross sections. The OBKN calculations are known to overestimate the capture cross-section data by an order of magnitude. The calculated values in this approximation with a scaling factor of 0.1 do not explain the data at all energies. Lapicki and Losonsky [26], starting from OBKN formula, have calculated in the second Born approximation the cross sections for electron capture from inner atomic shells of a target atom by fully stripped ions of velocities high compared to the electron velocities of inner shells of the target atom. For ions of low velocity the effects of binding and Coulomb deflection have also been

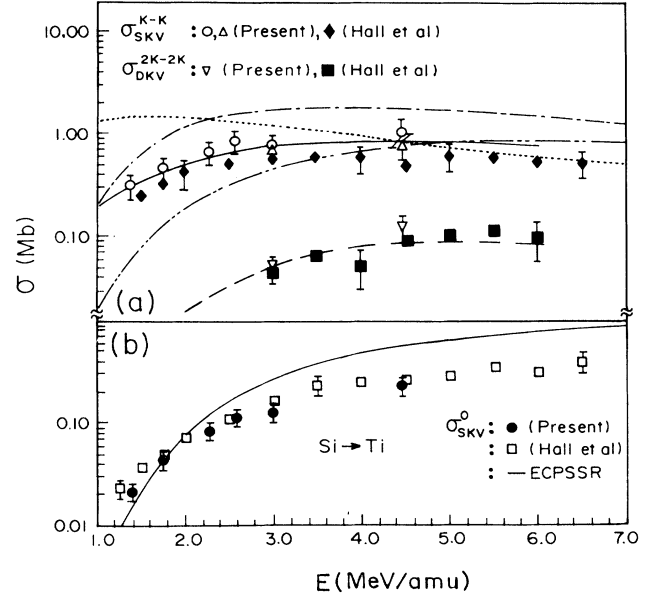


FIG. 4. (a) The single K - K electron transfer (σ_{SKV}^{K-K}) and double K - K electron transfer (σ_{DKV}^{2K-2K}) cross sections for the ^{28}Si beam on Ti. The values of Hall *et al.* were taken from Ref. [8]. The continuous (dashed) line represents the AO+ model calculations [12] for σ_{SKV}^{K-K} (σ_{DKV}^{2K-2K}). The dashed-dotted line and the dashed-dotted-dotted line correspond to the K - K capture cross sections calculated using the formulations given in Refs. [11] and [26], respectively. The dotted line denotes the calculations using the OBKN formulation (see text) with a normalization factor 0.1. (b) the single- K -vacancy direct-ionization cross sections for incident beam with zero vacancy in the K shell σ_{SKV}^0 .

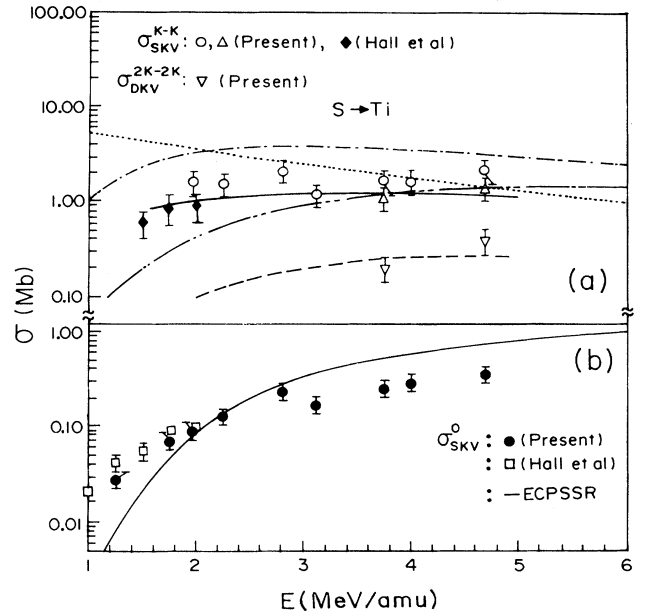


FIG. 5. (a) The single (σ_{SKV}^{K-K}) and double (σ_{DKV}^{2K-2K}) K - K -electron transfer cross sections for the ^{32}S beam on Ti. The lines have the same meaning as in Fig. 4(a). (b) The single- K -vacancy direct-ionization cross sections for incident beam with zero vacancy in the K shell σ_{SKV}^0 . The lines have the same meaning as in Fig. 4(b).

included. Both these results at low and high velocity were joined through an expedient interpolation formula. The calculated values underestimate the measured data but they reproduce the energy dependence quite well. Lapicki and McDaniel [11] have modified the above approach so that the binding effect was reduced (due to the introduction of the radial cutoff). The calculated cross sections, however, overestimate the data by a factor of ≈ 2 but again it explains the data only qualitatively. Both the K - K as well as the $2K$ - $2K$ capture cross-section data are best explained by the $AO+$ model calculations [13,14] for both the systems. For S data we have used the calculated values provided by Lin [27]. For Si data these calculations were taken from Refs. [8,9].

The enhancement factors $\alpha_{SKV}(\sigma_{SKV}^1/\sigma_{SKV}^0)$ for single K -vacancy production at various beam energies are shown in Fig. 6. We have calculated this quantity by using the cross sections calculated in the $AO+$ approximation for σ_{SKV}^{K-K} and the ECPSSR values for σ_{SKV}^0 . It can be expressed in the following form:

$$\alpha_{SKV} = 1 + \sigma_{SKV}^{K-K}(AO+) / \sigma_{SKV}^0(ECPSSR). \quad (10)$$

The calculated values are shown in Fig. 6 by a continuous line for ^{28}Si . The inset in Fig. 6 shows similar data for the ^{32}S beam. The agreement between the calculated and the measured values is good above 2 MeV/amu below which they overestimate the measured data. Below 2 MeV/amu the calculated values of α_{SKV} decrease very rapidly with increasing energy. This is due to the fact that the ECPSSR values increase very sharply whereas the $AO+$ values vary rather slowly in this energy range (see Figs. 4 and 5).

In the present case, since v_1/v_{2K} varies between 0.24 to 0.73 (representing a low-to-intermediate energy range), one can also calculate σ_{SKV}^{K-K} and α_{SKV} , using the work of Meyerhof [28] and Taulbjerg *et al.* [29] as demonstrated by Gray *et al.* [30]. In this method the single- K -vacancy production cross section with single- K -vacancy in the incident beam (σ_{SKV}^1) is given by

$$\sigma_{SKV}^1 = (\sigma_{SKV}^0 + \pi R^2 W) / \sigma_{SKV}^0, \quad (11)$$

where the second term in the bracket is nothing but the K - K capture cross section. The quantity W represents the Meyerhof single pass electron transfer probability and is given by

$$W = \frac{1}{1 + \exp(2|\chi|)}, \quad (12)$$

where

$$\chi = \frac{13.6}{(v_1/v_0)} \frac{I_1 - I_2}{I_2^{1/2} + I_1^{1/2}}. \quad (13)$$

In this expression I_1 and I_2 are the K -shell binding energies for the target and the one-electron ion, respectively, and $v_0 = c/137$. The quantity πR^2 is the geometrical cross section at a radius R for which the dynamical coupling element is the maximum. Its value can be found in Ref. [29]. The scaled value of R , i.e., R/Z_2 , was used for the corresponding $Q(=Z_2/Z_1)$ [29]. The calculated values of α_{SKV} in this approximation are shown in Fig. 6 as a dashed line. The measured values of σ_{SKV}^0 were used for these calculations. The hatched region represents the errors in the calculated values which arise mainly due to the error in the measured values of σ_{SKV}^0 . The energy dependence of this quantity is reproduced quite well in this model though it underestimates the data by about 10–40%. The agreement was found to be better for the Si data compared to the S data. It can be easily seen that in the low energy region this approximation (dashed line) gives a better estimate of α_{SKV} as compared to the earlier method as described above [see Eq. (10)] (continuous line). Gray *et al.* [30] have reported a very good agreement between their measured value of α_{SKV} for the Cl beam (of 60 MeV) on Cu and the calculated values in this model. The K - K single-electron transfer cross sections ($\sigma_{SKV}^{K-K} = \pi R^2 W$) as calculated from this model are shown in Fig. 7 as the dashed lines. The calculated values reproduce the qualitative behavior quite well. Quantitatively it also gives a good agreement with the measured data though it underestimates the data (about 10–40%) for both the collision systems at all the energies.

The double- K -vacancy (DKV) production was significant for energies ≥ 3 MeV/amu. The DKV cross sections as well as the double K - K -electron transfer cross sections were determined from an analysis of the K -hypersatellite intensity as outlined in Eqs. (5)–(8). Table II contains these cross sections for both the projectiles. The charge state dependence of DKV as well as SKV cross sections are displayed in Fig. 8. The enhancement of the DKV cross sections for the bare ions is very prominent and this is due to the increase of the double K - K transfer from target to the projectile with empty K shell. The double K - K capture cross sections (σ_{DKV}^{2K-2K}) are extracted for both the projectiles at a few energies ≥ 3 MeV/amu. The measured data are shown in Figs. 4 and 5. The agreement with the $AO+$ model calculations is excellent. The ratio of $\sigma_{DKV}^i/\sigma_{SKV}^i$ for $i=0,1,2$ is plotted in Fig. 9. The data agree quite well with the general trend of the existing data [31] for Si on Ti. The rise in

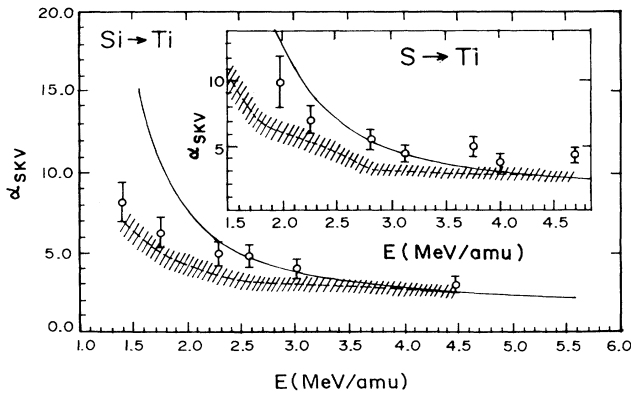


FIG. 6. The single- K -vacancy enhancement factor α_{SKV} for ^{28}Si on Ti derived in the zero thickness limit. The continuous (dashed) lines are the calculated values obtained using Eq. (10) [Eq. (11)]. The inset shows the similar quantities for ^{32}S on Ti (see text).

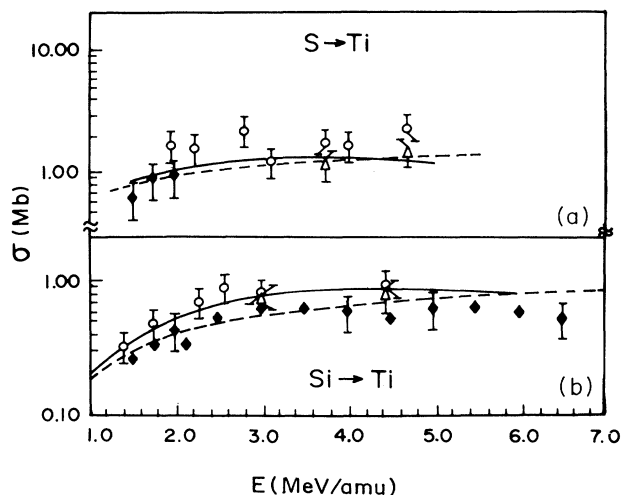


FIG. 7. The single K - K -electron transfer (σ_{SKV}^{K-K}) cross sections for ^{28}Si and ^{32}S on Ti, as in Figs. 4 and 5. The open symbols represent the present work and the closed ones are taken from Ref. [8]. The dashed lines in both (a) and (b) are the values calculated using Eq. (11) (see text). The continuous lines are the AO+ calculations as in Figs. 4 and 5.

this ratio for bare ions of S over that of Si is due to the increase in the double K - K transfer as the ratio Z_1/Z_2 approaches unity where the resonant charge transfer occurs.

The projectile cross sections of electron capture and loss (σ_{10} and σ_{01} , respectively) extracted from the fits of Eq. (3) to the experimental data (see Fig. 3) are shown in Fig. 10 as a function of the projectile energy. These cross sections are compared with existing theoretical models. The capture cross sections are compared with the prediction of the OBKN approximation using the formula given in Ref. [10]. The calculated cross sections include electron capture from the target (K, L, M) to projectile K shell. A reasonably good fit to the experimental data at all the energies can be obtained provided the OBKN cross sections are scaled uniformly by a factor of 0.15. The capture cross sections have also been calculated using the theory given by Lapicky and McDaniel [11]. The calculated values include the transfer cross sections from the target K, L to the projectile K shell. The calculated cross sections are nearly a factor of 2 higher at all the en-

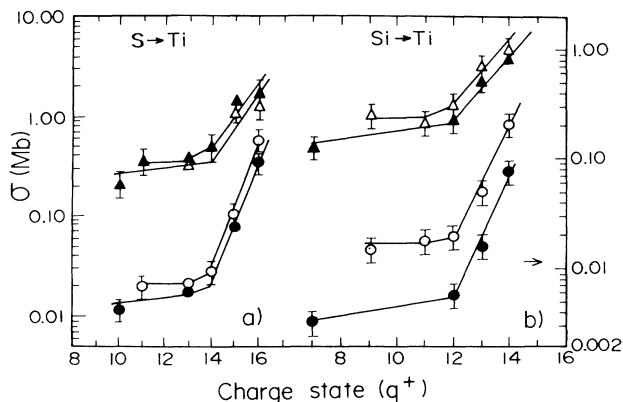


FIG. 8. The single- and double- K -vacancy cross sections for ^{32}S and ^{28}Si on Ti as a function of beam charge states. The data for various beam energies are shown. All the circles and the triangles denote σ_{DKV} and σ_{SKV} , respectively. The open (closed) symbols represent the data for 120(150)-MeV S on Ti in (a) and 84(125)-MeV Si on Ti in (b). The lines joining the points are to guide the eye.

ergies.

The calculations for the projectile loss cross section in heavy ion collisions are much more complex. We have tried to understand the data qualitatively treating electron loss as an ionization process of the projectile electron caused by the target atom. We have calculated the loss cross sections for the present collision systems using PWBA (with the roles of the projectile and the targets reversed). These cross sections overestimate the loss cross sections but reproduce the energy dependence rather well for both the ions. Similar results are also reported in our previous work [15] on S-Gd collision system. The calculated values scaled by a common factor of 0.04 are shown in Fig. 10. The same scale factor does not explain the S and Si data. Such a discrepancy between the calculated values and the measured data may not be surprising as in these cases $Z(\text{Ti}) > Z(\text{S or Si})$ and for projectile ionization, as in the present case, PWBA is supposed to be applicable in the reversed situation. The effective charge (q_T^*) of the ionizing particle (Ti atom) is also uncertain (see p. 113 of Ref. [6]). Similar discrepancies between the measured and calculated values for oxygen ions on different targets are also reported by Boman, Bernstein, and Tanis [32].

TABLE II. The double- K -vacancy cross sections of Ti for ^{28}Si and ^{32}S beams. All cross sections are in units of Mb. The average errors in σ_{DKV}^{2K-2K} are about 33%.

Beam	E (MeV/amu)	σ_{DKV}^0	σ_{DKV}^1	σ_{DKV}^2	σ_{DKV}^{2K-2K}
Si	3.00	0.00342	0.0163	0.0807	0.0515
	4.46	0.0154	0.0506	0.210	0.125
S	3.75	0.012	0.079	0.346	0.200
	4.00	0.016	0.083		
	4.69	0.017	0.107	0.589	0.392

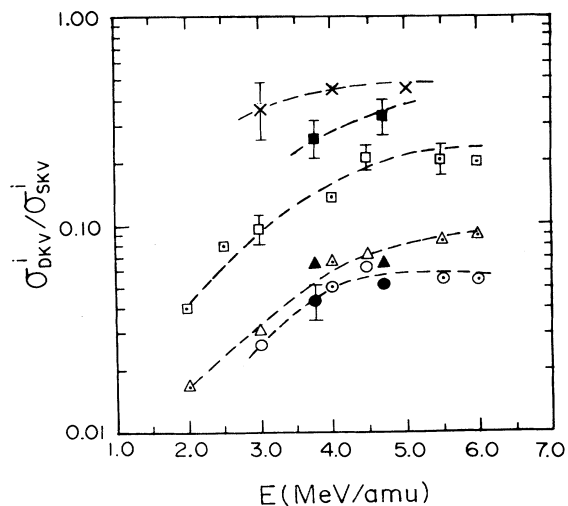


FIG. 9. The ratio $\sigma_{DKV}^i/\sigma_{SKV}^i$ are plotted for Si and S on Ti. The superscript i ($=0, 1, 2$) corresponds to the number of K vacancies in the incident beam. The open (closed) symbols are for the Si(S) beam. The circles, triangles, and squares are for multielectron ($q \geq Z_1 - 2$) ions, single-electron ($q = Z_1 - 1$) ions, and bare ($q = Z_1$) ions, respectively. The open symbols with dots at the center are taken from Ref. [31]. The dashed lines are to guide the eye. The crosses (x) correspond to the data for fully stripped Cl on Ti and are taken from Ref. [9].

IV. CONCLUSIONS

Single and double K - K -electron transfer and the K -shell-vacancy production cross sections have been measured for Ti bombarded by ^{28}Si and ^{32}S in the energy range 1.25–4.75 MeV/amu. The measurements using a ^{32}S beam beyond 2.25 MeV/amu are in a previously unmeasured region. The single and double K - K transfer cross sections are explained very well by the AO+ model [13,14]. The ECPSSR calculation underestimates the direct ionization cross-section data below 1.8 MeV/amu and overestimates above 3 MeV/amu. The enhancement

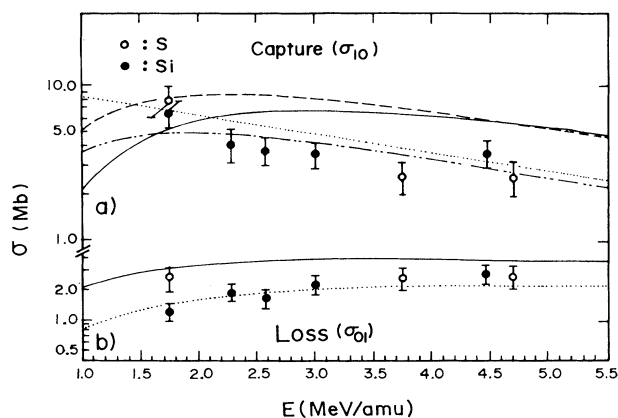


FIG. 10. The projectile cross sections for single-electron capture (σ_{i0}) (a) and loss (σ_{0i}) cross sections (b). The dotted and the continuous lines in (b) correspond to PWBA calculations for S and Si on Ti, respectively, with a normalization factor of 0.04 (see text). The dotted and the dashed-dotted lines in (a) correspond to the OBKN calculation for S and Si on Ti, respectively, with a normalization factor of 0.1. The dashed and the continuous lines correspond to capture calculations by Lapicki and McDaniel [11] for S and Si, respectively.

factor α_{SKV} can also be understood in terms of the formulations of Meyerhof [28] and Taulberg, Vabeen, and Fastrup [29].

ACKNOWLEDGMENTS

The authors thank C. D. Lin and Z. Chen for providing the calculations for the K - K and $2K$ - $2K$ transfer cross sections reported in this work and P. Richards for communicating the results of S-Ti and Si-Ti systems. They also thank Vandana Nanal, M. B. Naik, and D. C. Karve for help during the measurement and D. C. Ephraim for the preparation of carbon foils. The help of the operators for smooth running of the accelerator is gratefully acknowledged.

- [1] For a review see G. Lapicki, *J. Phys. Chem. Ref. Data* **18**, 111 (1989); H. Paul and J. Sacher, *At. Data Nucl. Data Tables* **42**, 106 (1989); H. Paul and J. Muhr, *Phys. Rep.* **135**, 47 (1986).
- [2] Y. C. Yu, M. R. McNeir, D. L. Weathers, J. L. Duggan, F. D. McDaniel, and G. Lapicki, *Phys. Rev. A* **44**, 5702 (1991).
- [3] L. C. Tribedi and P. N. Tandon, *Phys. Rev. A* **45**, 7860 (1992); **46**, 4425 (1992).
- [4] Y. C. Yu, M. R. McNeir, D. L. Weathers, J. L. Duggan, F. D. McDaniel, D. K. Marble, Z. Y. Zhao, and G. Lapicki, *Phys. Rev. A* **44**, 7252 (1991).
- [5] W. Brandt and G. Lapicki, *Phys. Rev. A* **23**, 171 (1981) and references therein.
- [6] See, e.g., T. J. Gray, in *Methods of Experimental Physics*, edited by P. Richard (Academic, New York, 1980), Vol. 17, p. 193.
- [7] J. A. Tanis, S. M. Shafroth, W. W. Jacobs, T. McAbee, and G. Lapicki, *Phys. Rev. A* **31**, 750 (1985).
- [8] J. Hall, P. Richard, T. J. Gray, N. Newcomb, P. Pepmiller, C. Dolin, K. Jones, B. Johnson, and D. Gregory, *Phys. Rev. A* **28**, 99 (1983).
- [9] J. Hall, P. Richard, P. L. Pepmiller, D. C. Gregory, P. D. Miller, C. D. Moak, C. M. Jones, G. D. Alton, L. B. Bridwell and C. J. Sofield, *Phys. Rev. A* **33**, 914 (1986).
- [10] V. S. Nikolaev, *Zh. Eksp. Teor. Fiz.* **51**, 1263 (1966) [*Sov. Phys. JETP* **24**, 847 (1967)].
- [11] G. Lapicki and F. D. McDaniel, *Phys. Rev. A* **22**, 1896 (1980).
- [12] C. D. Lin and L. N. Tunnell, *Phys. Rev. A* **22**, 76 (1980) and references therein.
- [13] W. Fritsch and C. D. Lin, *J. Phys. B* **15**, 1255 (1982); **15**, L281 (1982); *Phys. Rev. A* **26**, 762 (1982).
- [14] W. Fritsch and C. D. Lin, *Phys. Rep.* **202**, 1 (1991).
- [15] L. C. Tribedi, K. G. Prasad, and P. N. Tandon, *Z. Phys. D* **24**, 215 (1992).

- [16] S. D. Narvekar, R. R. Hosangdi, L. C. Tribedi, R. G. Pillay, K. G. Prasad, and P. N. Tandon, *Pramana* **39**, 79 (1992).
- [17] L. C. Tribedi, S. D. Narvekar, R. G. Pillay, and P. N. Tandon, *Pramana* **39**, 661 (1992).
- [18] L. C. Tribedi and P. N. Tandon, *Nucl. Instrum. Methods B* **62**, 178 (1992).
- [19] M. O. Krause, *J. Phys. Chem. Ref. Data* **8**, 307 (1979).
- [20] J. H. Scofield, *Phys. Rev. A* **9**, 1041 (1974).
- [21] F. P. Larkins, *J. Phys. B* **4**, L29 (1971).
- [22] J. M. Hall, Ph.D. thesis, Kansas State University, 1981 (unpublished).
- [23] S. K. Allison, *Rev. Mod. Phys.* **30**, 1137 (1958).
- [24] R. K. Gardner, T. J. Gray, P. Richard, C. Schmiedekamp, K. A. Jannison, and J. M. Hall, *Phys. Rev. A* **15**, 2202 (1977).
- [25] Ann Schmiedekamp, Tom J. Gray, B. L. Coyle, and U. Schiebel, *Phys. Rev. A* **19**, 19 (1979).
- [26] G. Lapicki and W. Losonsky, *Phys. Rev. A* **15**, 896 (1977).
- [27] C. D. Lin (private communication).
- [28] W. E. Meyerhof, *Phys. Rev. Lett.* **31**, 1341 (1973).
- [29] K. Taulbjerg, J. Vabeen, and B. Fastrup, *Phys. Rev. A* **12**, 2325 (1975).
- [30] T. J. Gray, P. Richard, K. A. Jamison, J. M. Hall, and R. K. Gardner, *Phys. Rev. A* **14**, 1333 (1976).
- [31] C. D. Lin and Patrick Richard, in *Advances in Atomic and Molecular Physics*, edited by D. Bates and B. Bederson (Academic, New York, 1981), Vol. 17, p. 275.
- [32] S. A. Boman, E. M. Bernstein, and J. A. Tanis, *Phys. Rev. A* **39**, 4423 (1989).